Research Article

Standalone Velocity Estimation Method for BDS Receiver Based on Improved ARUKF

Zilong Shen, **Wenxiang Liu**, **Jing Peng, Feixue Wang**, **and Wei Xiao**

College of Electronic Science, National University of Defense Technology, Changsha 410073, China

Correspondence should be addressed to Wenxiang Liu; liuwenxiang8888@163.com

The Carrier-Phase-Derived Doppler (CPDD) observation is an important type of observation for high-precision standalone velocity estimation (SVE) with the BeiDou Navigation Satellite System (BDS) receiver. The CPDD observation is susceptible to receiver clock jump, carrier-phase cycle slips, and multipath error. How to improve the accuracy and reliability of the SVE method based on the CPDD observation has become an urgent problem to be solved. Based on the Velocity Domain Selective Fusion (VDSF) strategy, this paper proposes the VDSF-ARUKF method for accuracy and reliability improvement of the SVE results of the original ARUKF method. In this improved ARUKF method, the CPDD observation and the raw Doppler observation are fused together based on the detection statistic under the framework of the Adaptively Robust Unscented Kalman Filter (ARUKF). Based on actual observations of the BDS receiver, a set of testing experiments were designed to verify the effectiveness of this improved ARUKF method. The experimental results show that the SVE method of the BDS receiver based on the VDSF-ARUKF can improve the accuracy and reliability of the ARUKF SVE results of the BDS receiver. In the case of multidimensional gross errors in the CPDD observations, the VDSF-ARUKF method can still obtain the SVE results with the highest accuracy on the order of several 10^{-2} m/s when compared with the VDFF-ARUKF method and the ARUKF method using the CPDD observations.

1. Introduction

Velocity is one of the most basic navigation information provided by the satellite navigation receivers. In application scenarios such as aircraft control and weapon testing [1], more accurate velocity information is needed. Accurate velocity information of the dynamic carrier is often required in applications such as navigation solution under highly dynamic condition, airborne gravimetry [2, 3], GNSS/INS integrated navigation, and geophysical exploration [4, 5]. At the same time, in the dynamic standalone velocity estimation scene, it is often affected by the challenging environment such as frequent signal obstruction and weak signal observation conditions [6, 7]. If the error suppression method and information fusion method are used unreasonable for the gross error suppression and elimination, the reliability and accuracy of the dynamic velocity estimation results of the navigation receiver will be greatly reduced [8]. Therefore, it is necessary to select appropriate error suppression methods and accuracy improvement methods, such as improving

the geometric observation conditions and improving the accuracy of the Doppler observation [9].

At present, the BeiDou Navigation Satellite System, one of the four Global Navigation Satellite Systems (GNSS), has been providing positioning, navigation, and timing functions for the Asia-Pacific region. As the BeiDou Navigation Satellite (Global) System is currently under construction [10], the number of visible navigation satellites of the BDS receiver is relatively small compared with that of the GPS receiver, and the corresponding observation geometry condition is weak. In particular, there are factors such as "urban canyon" in the dynamic SVE scene and tree occlusion in the vehicle navigation. The number of available carrier-phase observations is limited, and the number of the corresponding CPDD observations is also restricted. The robust filtering method is simpler and more applicable than the detection and direct elimination method of the gross errors. In particular, for the automatic control application scenarios, the motion control system of the dynamic carrier requires the velocity estimation results of the BDS receiver to maintain high

continuity and high availability. The output of the positioning and velocity estimation results needs to meet a certain update rate [11], which puts higher requirements on the gross error suppression ability of the SVE method.

When using a satellite navigation receiver for the SVE, the noise of the CPDD observations is usually very small. However, the CPDD observations are easily affected by the receiver clock jump [9], the gross errors in the carrier-phase observations, and the carrier-phase cycle slips [5]. Due to the lack of definite reference, it is impossible to judge whether the CPDD observations can be accurately repaired. In the real-time navigation solution, the corresponding CPDD observations are directly eliminated according to the strategy of direct detection with no repair. This will reduce the number of observations, affect the geometry distribution of visible navigation satellites, and cause the DOP value of the SVE to become too large, and the SVE process is no longer stable. However, the data quality of the raw Doppler observation is relatively stable. For the accuracy and reliability improvement of the SVE results, how to choose a reasonable data fusion method to fuse the raw Doppler observation and the CPDD observation is an important issue [5].

In recent years, there have been some researches on the SVE of the satellite navigation receiver. The basic velocity estimation methods used by the GNSS users can be summarized as follows: the position difference velocity estimation method, the CPDD velocity estimation method, and the raw Doppler velocity estimation method [1]. The analysis results indicate that the accuracy of the position difference velocity estimation method can reach the order of several 10^{-1}m/s, while the CPDD velocity estimation accuracy can reach the order of several 10^{-3}m/s [12]. These three velocity estimation methods have their own advantages, respectively, and it is impossible to blindly think which velocity estimation method is the best. The velocity estimation accuracy of the position difference velocity estimation method and the CPDD velocity estimation method is greatly influenced by the motion state of the carriers [13]. Relatively speaking, the raw Doppler velocity estimation method mainly depends on the accuracy of the Doppler observations and is basically not affected by the motion state of the carrier, so this method is highly recommended by the industry. Scholars have done a lot of research on the accuracy analysis of the positioning services that the BDS receivers can provide, but there are relatively few literatures on the accuracy analysis of the BDS standalone velocity estimation methods. Related research mainly focuses on the accuracy analysis of the standalone velocity estimation and analyzes various GPS velocity estimation methods [13, 14]. However, for the GPS and the BDS, the signal system, the observation accuracy, and the geometric distance between the satellites and the users have different characteristics [15, 16]. It is necessary to evaluate the SVE method based on the BDS system through the actual test [17]. The results of static data simulation test show that the accuracy of the velocity estimation using the raw Doppler observation is generally on the order of several 10^{-1}m/s ~ several 10^{-2}m/s, while the accuracy of the method using the CPDD observation is the highest, on the order of several 10^{-3}m/s [17, 18]. Using the

first-order central difference method to generate the CPDD observation can meet the requirements of the high-precision velocity estimation [19]. However, there are inevitably some cycle slips and gross errors in the carrier-phase observations [5, 8]. At present, the use of multifrequency observation can detect most of the cycle slips or gross errors with the magnitude of more than one cycle [20], but it is difficult to detect and correct small cycle slips and gross errors. Especially for the single-frequency navigation receivers, it is more difficult to perform quality control of the carrier-phase observations. These errors can reduce the accuracy of the SVE based on the CPDD observations to the order of several m/s ~ several 10^{-1}m/s. Of course, the raw Doppler observations are more noisy than the CPDD observations [21]. Based on the existing research listed above, whether the data fusion of the raw Doppler observation and the CPDD observation can improve the accuracy and reliability of the SVE method is a problem worthy of further study. Aiming at solving this problem, with the detection statistic of the residual error of the ARUKF method as the key parameter for data fusion in the velocity domain, we proposed an improved ARUKF method for standalone velocity estimation.

This article is organized as follows. In Section 2, based on the theory of robust filtering and the domain-based filtering strategy, the ARUKF filtering method is applied to the standalone positioning and velocity estimation. The shortcomings of the robust filtering method are analyzed. Based on the Velocity Domain Selective Fusion (VDSF) strategy, an improved ARUKF method of SVE has been proposed. Section 3 gives the performance evaluation results of the SVE based on the ARUKF method and the performance evaluation results of the SVE based on Velocity Domain Fault-tolerant Federated (VDFF) ARUKF method. Based on the above two performance evaluation experiments, the verification of the VDSF-ARUKF method is carried out at the end of Section 3. In the final testing experiment with the CPDD observations containing the multidimensional gross errors, the reliability of the improved ARUKF method is verified by the comparison of the SVE results of different filter-based SVE methods. Finally, the conclusion is given in Section 4.

2. The VDSF-ARUKF Standalone Velocity Estimation Method Based on the Fusion of the Raw Doppler Observation and the Carrier-Phase-Derived Doppler Observation

2.1. The ARUKF Navigation Solution Method for the BDS Receiver. The UKF navigation solution [22, 23] is an important method for the dynamic navigation information processing of satellite navigation receivers. In the actual dynamic navigation information estimation method, the observation equations and system equations of the navigation system usually exhibit nonlinear characteristics [23]. The UKF filter directly utilizes a nonlinear model to avoid introducing linearization errors, thereby improving the accuracy of the filter-based navigation solution and eliminating the need to
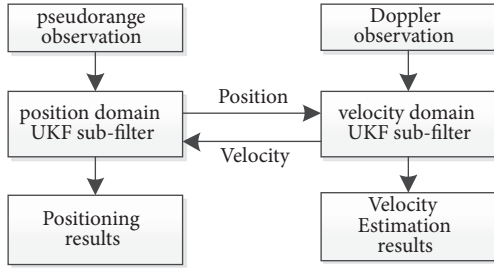
FIGURE 1: Flowchart of the domain-based ARUKF navigation solution method.

estimate the Jacobian matrix. Compared with the traditional EKF navigation solution method, when the system has non-linear characteristics, the UKF navigation solution method can improve the accuracy of the system state estimation. Apart from the requirement of an accurate system model by the EKF method, both the system noise and observation noise are zero-mean white Gaussian noise, which is often inconsistent with the actual situation. To solve this problem, the UKF navigation solution method is usually used. However, when using the classified adaptively robust filtering method [24, 25] in the UKF navigation solution, serious numerical stability problems arise. In order to improve the accuracy and reliability of the UKF navigation solution method and ensure the numerical stability of the UKF filter, the UKF subfilter is used in the position and velocity domain, respectively. The type of the subfilter is ARUKF filter.

The process of the ARUKF navigation solution method used in this paper is shown in Figure 1.

For the ARUKF navigation solution method, a subfilter is used in the position domain to process the pseudorange observations and obtain the standalone positioning results. In order to improve the accuracy of the positioning results, the velocity estimation result at each epoch is fed back into the position domain. In order to support the calculation of the filtering in the velocity domain, at the beginning of each epoch, the pseudorange observations are first used in the navigation solution to obtain the accurate positioning result, and the positioning result is then transferred to the subfilter in the velocity domain.

The key technology of the robust UKF filtering is to introduce the robust estimation theory into the adjustment model [26, 27], where the robust estimation is one of the focus areas of this paper. Through the robust estimation method, when the actual model of the system is consistent with the assumed model, the state estimation is optimal or near optimal. When there appears a small deviation between the actual model of the system and the assumed one, the estimation is less affected by the gross errors; when the actual model of the system deviates greatly from the assumed model, the state estimation is not seriously damaged [28].

Here we focus on the robust M estimation method, and the calculation steps of the robust M estimation in the UKF filter are given below. Suppose there is a set of independent observations $Z = \{z_i\}$, $i = 1, 2, \ldots, n$, the weight vector of the observations is $P = \{P_i\}$, and the error equations are shown

in (1). For the initialization of the observation weight vector P, the observation weight calculation method based on the elevation angle of the BDS satellites is used.

$$V = A\widehat{X} - Z \tag{1}$$

where Z is the observation vector, A is the measurement matrix, and V is the error vector.

Here, the calculation method of the robust solution is as shown in

$$\widehat{X} = \left(A^T \overline{P} A\right)^{-1} A^T \overline{P} Z \tag{2}$$

Here $\overline{P}$ is the robust equivalence weight matrix, whose elements represent the observation weights corresponding to the individual components in the observation vector Z. Through the principle of robust equivalence weight, the M estimation can be converted to a robust least square estimation, and the UKF filtering method uses the robust least square estimation to form a robust UKF filtering method.

In the ARUKF navigation solution method, the state discrepancy statistic is used as the discriminant statistic for calculating the adaptive factor [25], and then the adaptive factor is used to adjust the covariance matrix of the state vector in real time to control the influence of the dynamic model anomaly on the parameters. The method of calculating the adaptive factor is shown in

$$\overline{W}_k = \overline{x}_{k|k-1} - \widehat{x}_k \tag{3}$$

$$\Delta \overline{W}_k = \frac{\overline{W}_k}{\sqrt{\text{tr}\left(P_{\overline{W}_k}\right)}} \tag{4}$$

Here $\text{tr}(\cdot)$ is the symbol of matrix trace operation. $\overline{W}_k$ is the difference between the prediction of the state vector and the robust solution of the state vector. $\Delta \overline{W}_k$ is the standardized residual. $\overline{x}_{k|k-1}$ is the prediction of the state vector. $\widehat{x}_k$ is the robust solution of the state vector.

The adaptive factor α_k is implemented using the piecewise functions. The specific form is shown in

$$\alpha_k = \begin{cases} 1 & \Delta \overline{W}_k \leq c \\ \dfrac{c}{\left|\Delta \overline{W}_k\right|} & \left|\Delta \overline{W}_k\right| > c \end{cases} \tag{5}$$

Here c is the threshold constant when calculating the adaptive factor α_k, whose range is from 1.0 to 2.5. α_k is an adaptive factor at epoch k. $\Delta \overline{W}_k$ is the standardized difference between the prediction of the state vector and the robust solution of the state vector. When this difference is too large, the state of the system is abnormal.

The specific method to determine the robust equivalence weight matrix $\overline{P}$ is given below. For the initialization of the robust equivalence weight matrix $\overline{P}$, the observation weight calculation method based on the elevation angle of the BDS satellite is used. The subsequent adjustments of the robust equivalence weight matrix $\overline{P}$ are mainly based on the iteration process of the measurement update step. The adjustment

method of the robust equivalence weight in the iteration process is based on the Huber robust equivalent weight function. This method is based on the principle of variance expansion, and the calculation method of the inflation factor is as shown in (6).

The inflation factor is calculated based on the variance-expansion principle to resist the influence of the gross errors in the observations [26]. By constructing a robust inflation factor, we can establish an equivalence covariance matrix of the observation noise. At the same time, we can also obtain the robust equivalence weight matrix $\overline{P}$ of the navigation observations, because the covariance matrix of the observation noise can be seen as the inverse matrix of the robust equivalent weight matrix of the navigation observations. The covariance matrix of the observation noise reflects the dispersion degree of the navigation observations. If the observations have high accuracy and good reliability, the variance of the corresponding observations is small, and the weight of the observations in the state estimation is large. On the contrary, if the observation with low reliability contains gross errors, the variance of the corresponding observation will become large, and the weight of the observation in the state estimation process will be small. Therefore, by appropriately expanding the variance of the anomaly observations to reduce the influence of the gross errors on the state estimation, the reliability of the filter-based navigation solution method can be improved.

In the iteration process of the observation weight calculation, assuming that the observations are not correlated, and only the variance elements of the robust equivalence weight matrix $\overline{P}$ are considered, the original variance of the observation y_k is σ_k^2. If there are gross errors existing in the observations, then $\overline{\sigma}_k^2 = \beta_k \sigma_k^2$, where β_k is the inflation factor, and $\overline{\sigma}_k^2$ is the equivalence variance. $\overline{\sigma}_k^2$ can be used to calculate the elements of the robust equivalence weight matrix $\overline{P}$. The construction of variance inflation factor is shown in

$$\beta_k = \begin{cases} \dfrac{|V_k|}{c} & |V_k| \geq c \\ 1 & |V_k| < c \end{cases} \tag{6}$$

Here V_k is the residual of the prediction value, c is the threshold constant when calculating the variance inflation factor. Here, as the discriminant criterion of gross errors, take $c = 3\sigma_0^2$, where σ_0^2 is the variance of observation noise. By using the variance inflation factor β_k, when there is gross error in the observation, that is, when the error of the observation exceeds a certain threshold, the variance inflation calculation is performed. Conversely, the variance remains unchanged.

The calculation steps of the ARUKF filtering method are as follows:

(1) The ARUKF method is initialized by using the Weighted Least Square (WLS) method.

(2) The Sigma points in the process of time update are calculated, and the Sigma points are used to update the state

vector of the filter. The calculation method of the Sigma set is shown in (7). The number of the Sigma points is $2n + 1$.

$$\chi_{i,k-1} = \overline{X}_{k-1}^0 \quad i = 0$$

$$\chi_{i,k-1} = \overline{X}_{k-1}^0 + \left(\sqrt{(n + \lambda) P_{k-1}} \right)_i \quad i = 1, \ldots, n \tag{7}$$

$$\chi_{i,k-1} = \overline{X}_{k-1}^0 - \left(\sqrt{(n + \lambda) P_{k-1}} \right)_i \quad i = n + 1, \ldots, 2n$$

Here χ is the Sigma point. The solution of $\sqrt{(n + \lambda)P_{k-1}}$ is generally recommended to use the matrix Cholesky decomposition algorithm. The calculation method of λ is as shown in

$$\lambda = \alpha^2 (n + k) - n \tag{8}$$

Here α is the distance from the Sigma point to the mean of the state vector $\overline{X}$, the range of α is $10^{-4} < \alpha \leq 1$, and k is generally 0.

The corresponding weights of Sigma points are shown in

$$W_i^m = \frac{\lambda}{\lambda + n} \quad i = 0$$

$$W_i^{(c)} = \frac{\lambda}{\lambda + n} + \left(1 - \alpha^2 + \beta \right) \quad i = 0 \tag{9}$$

$$W_i^{(m)} = W_i^{(c)} = \frac{\lambda}{2 (\lambda + n)} \quad i = 1, \ldots, 2n$$

Here β contains the distribution information of the Sigma points. For the Gaussian, the value of β is 2. $W_i^{(m)} \geq 0$ means that the Sigma point is far away from the average of the state vector. $W_i^{(m)} \leq 0$ means that the Sigma point is close to the average of the state vector.

The process of time update is shown in

$$\chi_{k|k-1} = f(\chi_{k-1})$$

$$\widehat{x}_{k|k-1} = \sum_{i=0}^{2n} \left[W_i^{(m)} (\chi_{k|k-1})_i \right]$$

$$P_{k|k-1} = \sum_{i=0}^{2n} \left\{ W_i^{(c)} \left[(\chi_{k|k-1})_i - \widehat{x}_{k|k-1} \right] \right.$$

$$\left. \cdot \left[(\chi_{k|k-1})_i - \widehat{x}_{k|k-1} \right]^T \right\} + Q_k \tag{10}$$

$$z_{k|k-1} = h(\chi_{k|k-1})$$

$$\widehat{z}_{k|k-1} = \sum_{i=0}^{2n} \left[W_i^{(m)} (z_{k|k-1})_i \right]$$

Here $P_{k|k-1}$ is the variance of the predicted sample point, $\widehat{z}_{k|k-1}$ is the mean of the predicted observations, and $\widehat{x}_{k|k-1}$ is the mean of the predicted state vector. f is the system function and h is the observation function. Q_k is the covariance matrix of the system dynamic noise. W is the weight of Sigma points. χ_{k-1} is the Sigma point. k is the epoch number. i is the number of Sigma points.

(3) Calculate the Sigma points in the process of observation update.

(4) Use the calculation method of the adaptive factor α_k. Before calculating the adaptive factor, the robust equivalence weight matrix is calculated, and the specific calculation process is shown in

$$
\begin{aligned}
\overline{P}_{\widehat{z}_k} \\
= \frac{1}{\alpha_k} \\
\cdot \sum_{i=0}^{2n} \left\{ W_i^{(c)} \left[(z_{k|k-1})_i - \widehat{z}_{k|k-1} \right] \left[(z_{k|k-1})_i - \widehat{z}_{k|k-1} \right]^T \right\} \\
+ R_k \\
P_{\widehat{z}_k} \\
= \sum_{i=0}^{2n} \left\{ W_i^{(c)} \left[(z_{k|k-1})_i - \widehat{z}_{k|k-1} \right] \left[(z_{k|k-1})_i - \widehat{z}_{k|k-1} \right]^T \right\} \\
+ R_k \\
P_{x_k, y_k} \\
= \sum_{i=0}^{2n} \left\{ W_i^{(c)} \left[(\chi_{k|k-1})_i - \widehat{x}_{k|k-1} \right] \left[(z_{k|k-1})_i - \widehat{z}_{k|k-1} \right]^T \right\} \\
\overline{K}_k = \frac{1}{\alpha_k} \cdot P_{x_k, y_k} \overline{P}_{\widehat{z}_k}^{-1} \\
\widehat{x}_k = \widehat{x}_{k|k-1} + \overline{K}_k \left(z_k - \widehat{z}_{k|k-1} \right) \\
P_k = \frac{1}{\alpha_k} \cdot P_{k|k-1} - \overline{K}_k P_{\widehat{z}_k} \overline{K}_k^T
\end{aligned}
\tag{11}
$$

Here R_k is the covariance matrix of the observation noise. $P_{k|k-1}$ is the variance of the predicted sample point. P_{x_k, y_k} and $P_{\widehat{z}_k}$ are the covariance matrix and variance matrix of the predicted observations. $\widehat{x}_{k|k-1}$ and $\widehat{z}_{k|k-1}$ are the mean values of the Sigma sets of state equations and observation equations, respectively. α_k is the adaptive factor at epoch k. $\overline{K}_k$ is the filtering gain. z_k is the observation value. $W_i^{(c)}$ is the weight of the Sigma point. k is the epoch number. i is the Sigma point number.

The algorithm flow of the ARUKF subfilter is shown in Figure 2.

Each subfilter is installed in the position domain for standalone positioning and in the velocity domain for standalone velocity estimation, which can ensure that the ARUKF filter is stable while utilizing the advantages of UKF filter's nonlinear characteristics at the same time. The test statistic based on the discrepancy value of the state is used to determine whether adaptive filtering is needed, and the prediction residual is used in determining whether the robust filtering based on the variance inflation method is required. When adaptive filtering and robust filtering are not required, the ARUKF filter for navigation solution degrades to a standard UKF filter.

An ARUKF subfilter is set in the position domain and velocity domain, respectively. For the position domain ARUKF subfilter, the corresponding state vector is the carrier's 3D position and the receiver clock bias; for the velocity domain ARUKF subfilter, the corresponding state vector is the carrier's 3D velocity and the receiver clock drift. Compared with the ARUKF navigation solution method both in the position domain and in velocity domain, the length of each subfilter's state vector is reduced by half, which improves the reliability of the ARUKF navigation solution method. At the same time, the standalone positioning result and SVE result at current epoch are exchanged between the position domain ARUKF subfilter and the velocity domain ARUKF subfilter, which can guarantee the accuracy of the navigation solution in both of the two subdomains.

2.2. The VDSF-ARUKF Standalone Velocity Estimation Method. When the carrier with the BDS receiver is in the state of low or middle dynamic motion, the accuracy of velocity estimation by the CPDD observation is much higher than that of the raw Doppler observation. However, when the BDS receiver is in the environment of frequent signal occlusion and weak signal, the CPDD observation, if affected by the harsh navigation signal environment, may have problems such as continuous cycle slips and gross errors. At this time, the accuracy of the generated CPDD observation is lower than that of the raw Doppler observation, and it is prone to the case where the CPDD observation cannot be calculated.

When the carrier-phase observations encounter clock jump, cycle slips, and multipath error, abrupt deviation could occur in the calculation of the CPDD observation. The commonly used gross error detection and inhibition methods include the robust filtering method, the innovation χ^2 detection method [29, 30], and the residual χ^2 detection method [31]. The robust equivalence weight matrix needs to be constructed in the robust filtering method. The existing methods of calculating the robust equivalence weight matrix under selection include Huber function, Hampel function, Turkey function, Andrews function, Danish weight function, and IGG scheme weight function. The Huber function [5, 32, 33] is adopted to construct the ARUKF method in this paper. The reason is that the Huber function is simpler to be implemented and the threshold setting of the robust filtering method is relatively simple. However, this method cannot directly eliminate the relatively large gross errors but can only inhibit the influence of the gross errors on the accuracy of the filtering method. Although it can improve the accuracy of the SVE in the case of small gross errors, it will make the ARUKF method based on the CPDD observations unable to resist the influence of large gross errors. In order to solve this problem, based on the principle of residual χ^2 detection method, a test statistic based on the residual of the Doppler observation is constructed in this paper. Based on this statistic, the raw Doppler velocity estimation result or the CPDD velocity estimation result can be used selectively to obtain a velocity estimation result with high reliability. The calculation method of this selective statistic is as shown in
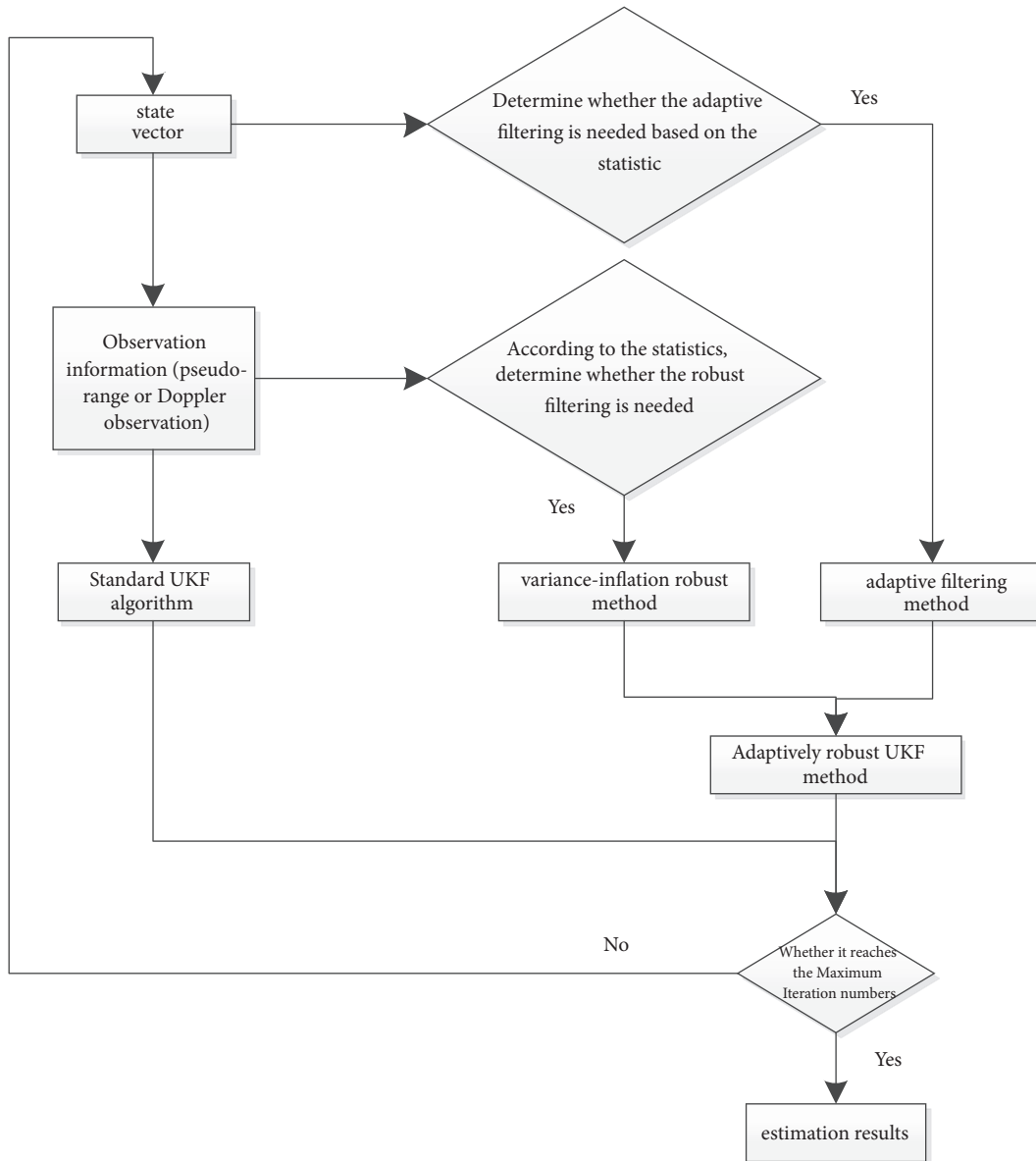
FIGURE 2: Algorithm flow of the ARUKF subfilter.

$$v = \left(v_1, v_2, v_3, \ldots v_m\right)^T \qquad (12)$$

$$\lambda(k) = \frac{v^T R(k) v}{(m - n - 1)}, \quad m - n - 1 > 0 \qquad (13)$$

Here v is the observation residual vector in the velocity domain. n is the dimension of the state vector. m is the number of the observations in the velocity domain. k is the epoch number. $R(k)$ is the covariance matrix of the observation noise at epoch k. $\lambda(k)$ is used as both the fault detection statistic at epoch k and the selective fusion statistic in the velocity domain, respectively. When the two subfilters in the velocity domain are used to estimate the velocity, the selective fusion statistic $\lambda(k)$ is calculated after the Doppler observation update. When $m - n - 1 \leq 0$, the navigation

solution result of the subfilter in the velocity domain is invalid at the current epoch, and the corresponding statistic $\lambda(k)$ of the subfilter is no longer calculated. When $m - n - 1 > 0$, the corresponding statistic $\lambda(k)$ of the subfilter is calculated and the fault detection for the velocity estimation result is made. In order to speed up this improved ARUKF method, once the fault is detected, it is directly determined that the navigation solution result of the current subfilter in the velocity domain is invalid, and the detection and isolation of the gross errors are not further performed; when the fault detection process is passed, the navigation solution result of the subfilter in velocity domain is sent to the selective fusion step. At this data fusion step, the result of the filtering using the CPDD observation or the result of the filtering using the raw Doppler observation is selected according to the selective
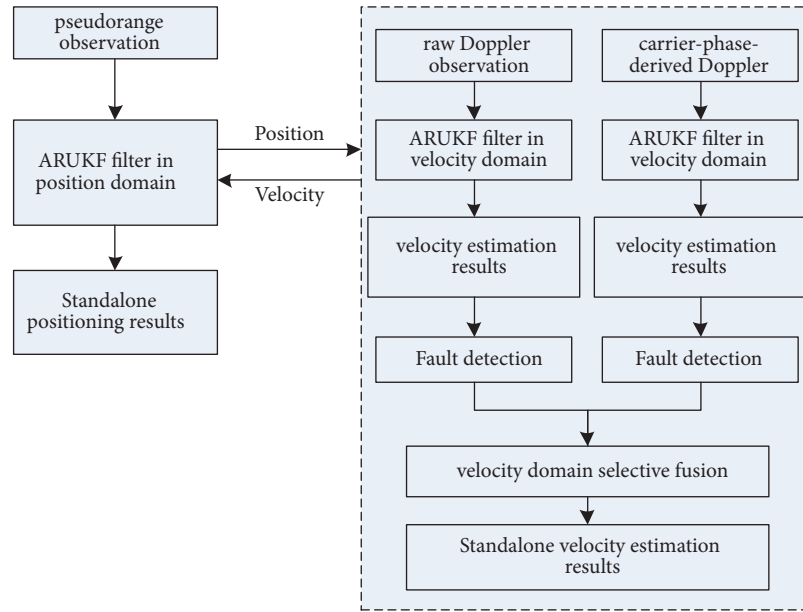
FIGURE 3: Structure diagram of the VDSF-ARUKF navigation solution method.

fusion statistic $\lambda(k)$. The structure of the proposed VDSF-ARUKF navigation solution method is shown in Figure 3.

The robust filtering method based on Huber robust equivalence weight function is combined with fault detection method based on the principle of residual χ^2 detection. Firstly, the robust filtering method is used to suppress the influence of small gross errors. Then the validity of the velocity estimation result of the subfilter is tested. The velocity estimation result with fault detected is directly judged to be invalid. Since two subfilters are used in the velocity domain, compared with the velocity estimation method using only one type of Doppler observation in the velocity domain, this method can effectively increase the availability of the SVE results. At the same time, the accuracy and reliability of the SVE results with this VDSF strategy are improved by combining the statistic of residual χ^2 detection.

For the improved ARUKF method based on the VDSF strategy proposed in this paper, the increase of the calculation amount is mainly due to the use of two sub-UKF filters in the velocity domain; that is to say, one more subfilter in the velocity domain is added compared with the standard UKF filter. However, considering that the length of the domain-based ARUKF filter's state vector is short, the increased calculation amount is not large. And the number of the calculation steps of the VDSF strategy is not large, so it can be seen as follows: the reliability of high-precision SVE is improved by increasing a small amount of the calculation. In order to reduce the calculation amount while maintaining the high accuracy and reliability of the improved ARUKF method, the following strategies are used: Firstly, the calculation amount of the ARUKF filter is controlled by setting the maximum iteration number of the observation update as small as possible. The second strategy is to reduce the calculation amount of adjusting the observation weight by

using the calculation method of the Huber robust equivalence weight, which is simpler to be implemented with the smaller calculation amount. Considering the practical need to increase the calculation speed for the real-time SVE and the increased performance of newly emerging embedded microprocessors, the added UKF subfilter does not cause a significant increase of the calculation amount. The contradiction between the calculation amount and the accuracy of the filtering navigation solution can be partially solved by the above strategies.

3. Results and Discussion

3.1. Performance Evaluation of the ARUKF Standalone Velocity Estimation Method. The VDSF-ARUKF navigation solution method proposed in this paper is the UKF filter based on the domain-based adaptively robust filtering strategy. In order to analyze the SVE performance of the VDSF-ARUKF method, the performance of the original ARUKF method was evaluated by using the actual experimental data. The experimental evaluation method is used to verify the effectiveness of the ARUKF method in the navigation solution method. The accuracy of the SVE results of the ARUKF method based on the CPDD observation is analyzed emphatically.

The car testing data collected in Guangzhou city is used to test the original ARUKF navigation solution method. The acquisition date of the observation data in the experiment was September 29, 2015, and the analysis and verification of this method were carried out using the real observation data of the dynamic car testing experiment. The adopted satellite navigation receiver is the self-developed BDS receiver with a sampling frequency of 1 Hz. The navigation solution method uses the observation of the BDS system, including the pseudorange observation, the carrier-phase observation,

TABLE 1: The SVE errors of 4 different ARUKF methods.

Method Type	Error Statistics				
	CEP (m/s)	SEP (m/s)	error components in the E, N, U directions (m/s)		
			E	N	U
ARUKF using raw Doppler observation	0.11	0.23	0.08	0.10	0.20
ARUKF using CPDD observation	0.10	0.12	0.02	0.16	0.05
VDFF-ARUKF	0.09	0.19	0.06	0.09	0.16
VDSF-ARUKF	0.04	0.06	0.02	0.06	0.03

and the raw Doppler observation of the same frequency. The first-order central difference method is used to generate the CPDD observation. The reference trajectory data of car testing experiment comes from the vehicle's GPS/INS integrated navigation system. The accuracy of the reference SVE results that can be output using the integrated navigation system is 0.03 m/s, and the error statistic of the velocity estimation used in the car testing experiment is RMS (95%).

$$\sigma_{err} = \sqrt{\left|v_{x_0} - v_{x_t}\right|^2 + \left|v_{y_0} - v_{y_t}\right|^2 + \left|v_{z_0} - v_{z_t}\right|^2} \qquad (14)$$

Here the reference velocity is $(v_{x_0}, v_{y_0}, v_{z_0})$ and the SVE result of the ARUKF navigation solution method is $(v_{x_t}, v_{y_t}, v_{z_t})$ in the ECEF coordinate system. Time of week is used to represent the corresponding epoch of the SVE result, and the corresponding time system is GPST. The error statistic CEP is used to describe the velocity estimation accuracy in the 2D horizontal direction, and the error statistic SEP is used to describe the velocity estimation accuracy in the 3D direction [34]. The raw Doppler observation and the CPDD observation are used, respectively, in the velocity domain. The SVE results are shown in Table 1, wherein when the CPDD observation is used in the velocity domain, the error statistic SEP is 0.12 m/s, and the error statistic CEP is 0.10 m/s. When observation used in the velocity domain is the raw Doppler observation, the error statistic SEP is 0.23 m/s, and the error statistic CEP is 0.11 m/s. When the observation used in velocity domain is the raw Doppler observation and the ARUKF method is used for the navigation solution, the SVE results in the X, Y, and Z directions of the ECEF coordinate system are shown in Figure 4. When the observation used in the velocity domain is the CPDD observation and the ARUKF navigation solution method is applied, the SVE results in the X, Y, and Z direction of the ECEF coordinate system are shown in Figure 5.

According to the SVE results in Table 1, when the ARUKF method in the velocity domain uses the raw Doppler or CPDD observation, the velocity estimation accuracy of these two methods in the 2D horizontal direction is basically the same. In the U direction of the ENU coordinate system, the error of velocity estimation using the CPDD observation is much smaller than that of using the raw Doppler observation, which indicates that the use of CPDD observation in the ARUKF navigation solution method can significantly improve the SVE accuracy in the vertical direction. In the 3D

direction of E, N, and U, according to the error statistic SEP of the velocity estimation results, when the CPDD observation is used for SVE, the accuracy of the velocity estimation is improved compared with that of using the raw Doppler observation by 0.1m/s. However, when using the CPDD observation, the SVE accuracy in the N direction of the ENU coordinate system is lower than the SVE accuracy using the raw Doppler observations. The possible reason is that there exist large gross errors in the CPDD observation, resulting in a decrease in the SVE accuracy in the N direction.

From the SVE results shown in Figure 4, it can be seen that in the ECEF coordinate system, the SVE results of the ARUKF method using the raw Doppler observation are worse in the X and Y direction than that in the Z direction, but it can still track the dynamic changes of the system in the 3D direction.

Comparing the SVE results of the ARUKF method using the CPDD observation shown in Figure 5, the velocity estimation errors in the X, Y, and Z directions are relatively smaller when using the CPDD observation. This method can track the dynamic change of the system well, but large errors in the SVE results occur at several epochs. The main reason may be that the CPDD observations are affected by the gross errors, resulting in the reduction of the geometric observation conditions, which will seriously affect the SVE results. From the SVE results of the ARUKF method using the raw Doppler observation in Figure 4, it can be seen that the SVE results of the ARUKF method using the CPDD observation are better than those of the ARUKF method using the raw Doppler observation in the X and Y directions of the ECEF coordinate system. At the same time, compared with the SVE results of the ARUKF method using the raw Doppler observation, the SVE results in the X, Y and Z directions when using the CPDD observations are relatively smoother, and the accuracy of the velocity estimation results at different epochs is more consistent.

3.2. Performance Evaluation of the VDFF-ARUKF Standalone Velocity Estimation Method.

Based on the ARUKF method, this paper uses the fault-tolerant federated filtering method to fuse the raw Doppler SVE results and the CPDD SVE results in the velocity domain. Here, the data of car testing collected in Guangzhou city is used to test and evaluate the Velocity Domain Fault-tolerant Federated ARUKF (VDFF-ARUKF) navigation solution method. The basic configuration of the test experiment is the same as the configuration in Section 3.1.
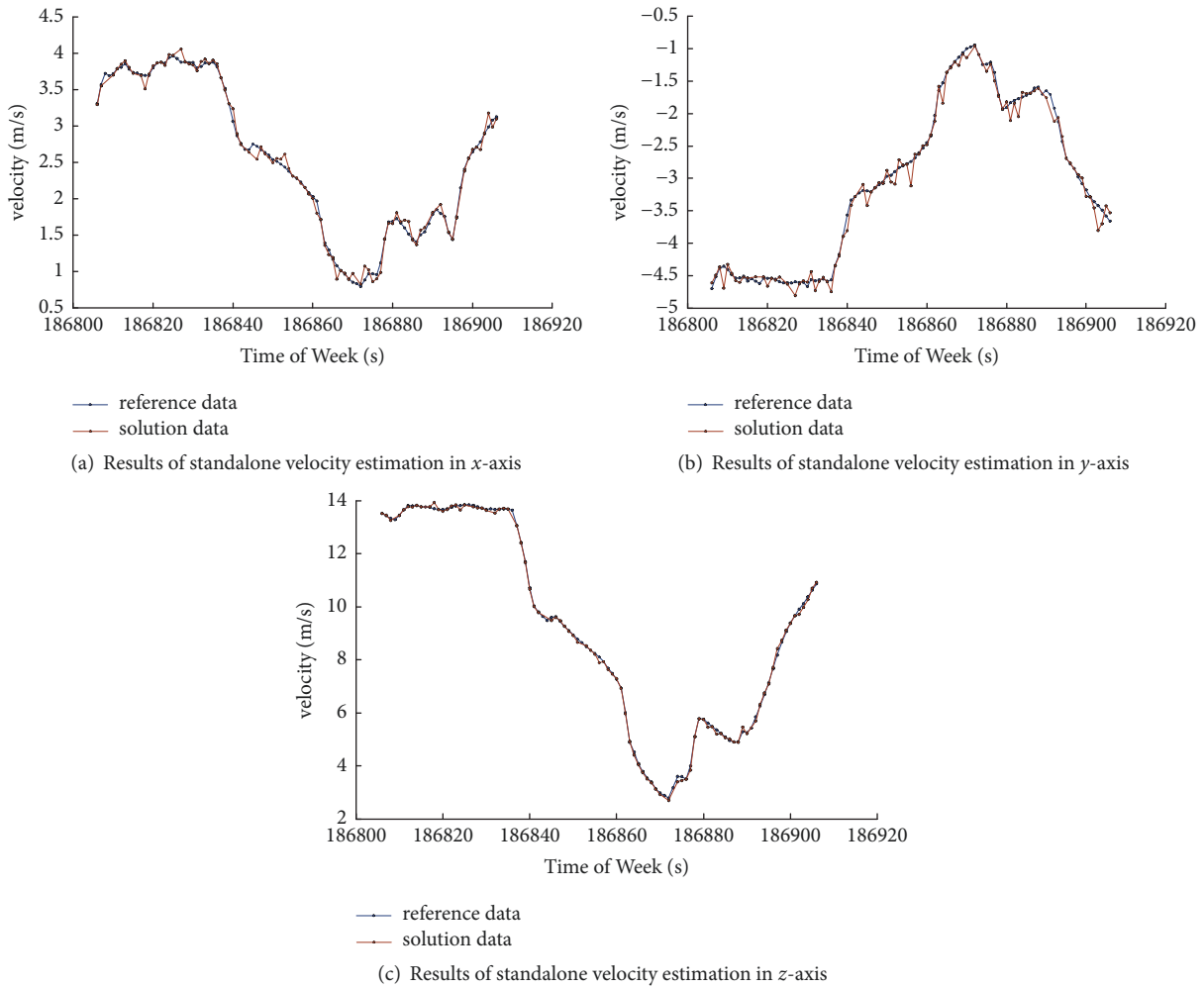
(a) Results of standalone velocity estimation in *x*-axis

(b) Results of standalone velocity estimation in *y*-axis

(c) Results of standalone velocity estimation in *z*-axis

FIGURE 4: Velocity estimation results of ARUKF method using raw Doppler observation in the *x*-, *y*-, and *z*-axis.

The accuracy of the VDFF-ARUKF method in the velocity domain is investigated by the experimental results. The accuracy evaluation indicators used are CEP, SEP, and RMS (95%). In the testing experiment, the accuracy of the reference SVE results that can be output using the integrated navigation system is 0.03 m/s. In the low-dynamic motion scene, the SVE accuracy of the VDFF-ARUKF method is evaluated separately in the 2D horizontal direction, in the 3D direction, and in the E, N, U directions of the ENU coordinate system.

Among the SVE results of dynamic station GZDT, the CEP, SEP, and the error statistics of the SVE in the E, N, and U directions of the ENU coordinate system are shown in Table 1. Here, the error statistic SEP in the 3D direction is 0.19 m/s, and the error statistic CEP in the 2D horizontal direction is 0.09 m/s. When the VDFF-ARUKF method in the velocity domain is used to perform the SVE, the SVE results in the X, Y, and Z directions of the ECEF coordinate system are shown in Figure 6.

Comparing the results in Table 1, it can be seen that the 3D velocity estimation error statistic SEP of the VDFF-ARUKF method in the velocity domain is higher than that of the ARUKF method using the raw Doppler observation. At the same time, the 3D velocity estimation error statistic SEP of the VDFF-ARUKF method in velocity domain is lower than that of the ARUKF method using the CPDD observation. And, in the N direction of the ENU coordinate system, the error statistic RMS of the VDFF-ARUKF navigation solution method is higher than that of the ARUKF method using the raw Doppler observation or the CPDD observation.

Comparing the SVE results in the X, Y, and Z directions shown in Figure 6, it can be seen that the VDFF-ARUKF navigation solution method in the velocity domain has a higher velocity estimation accuracy in the X and Z directions than that in the Y direction, and the velocity estimation result in the Y direction fluctuates greatly compared with the reference velocity. Compared with the results shown in Figures 6 and 5, it can be seen that the velocity estimation accuracy of the ARUKF navigation solution method using the CPDD observation is higher than that of the VDFF-ARUKF navigation solution method. However, at some time, due to the poor data quality of the CPDD observations, there is a large error in velocity estimation. At these epochs, the VDFF-ARUKF navigation solution method is not particularly sensitive to the data quality of the CPDD observations, because it

(a) Results of standalone velocity estimation in x-axis

(b) Results of standalone velocity estimation in y-axis

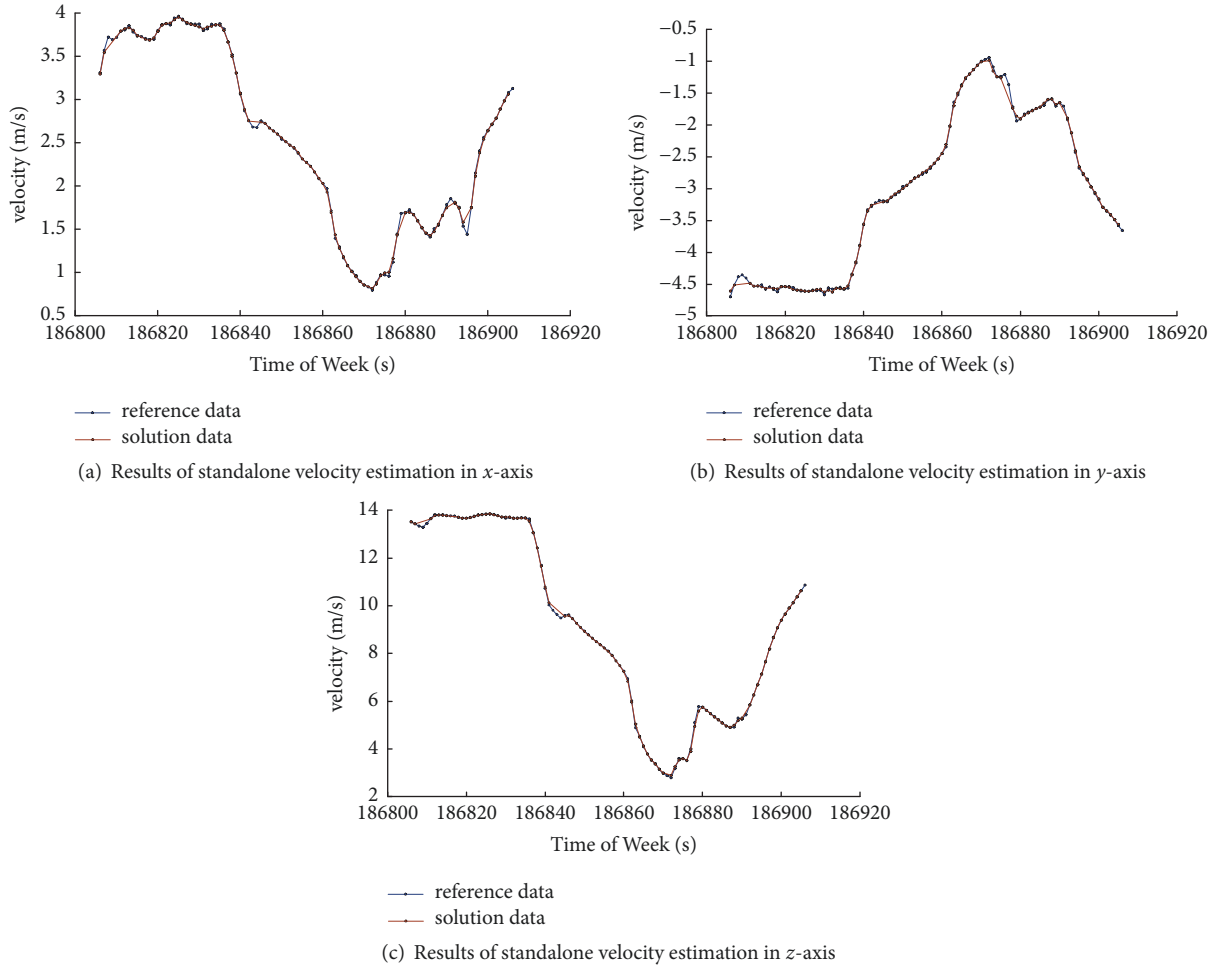(c) Results of standalone velocity estimation in z-axis

FIGURE 5: Velocity estimation results of the ARUKF method using the CPDD observation.

combines the raw Doppler SVE results. However, since the accuracy of the raw Doppler SVE is much lower than that of using the CPDD observation in low-dynamic scenes, this still makes the VDFF-ARUKF navigation solution method less accurate than the ARUKF navigation solution method using the CPDD observations.

3.3. Verification of the VDSF-ARUKF Standalone Velocity Estimation Method. According to the evaluation results of the VDFF-ARUKF navigation solution method in Section 3.2, the accuracy of the SVE can be partially improved by fusing the results of the raw Doppler velocity estimation and the CPDD velocity estimation based on the VDFF strategy. However, the overall accuracy of the velocity estimation is still lower than that of the original ARUKF navigation solution method using the CPDD observation.

The VDSF-ARUKF method was analyzed and verified by using the data of the dynamic car testing experiment in Guangzhou city. The basic configuration of the testing experiment is the same as the configuration in Section 3.1.

The accuracy of the SVE method is mainly investigated here. The accuracy evaluation indicators used in the test are CEP, SEP, and RMS (95%) [34]. In the testing experiment,

the accuracy of the reference SVE results that can be output using the integrated navigation system is 0.03 m/s. The 2D SVE accuracy and the 3D SVE accuracy in the low-dynamic motion scene are evaluated separately using the VDSF-ARUKF navigation solution method. The results in the X, Y, Z directions and the E, N, U directions are evaluated, respectively.

The SVE results of the dynamic station GZDT are statistically analyzed. The statistical results of CEP and SEP are shown in Table 1. The error statistic RMS of the SVE in the E, N, and U directions of the ENU coordinate system are also shown in Table 1. Among them, the SVE error statistic SEP in the 3D direction is 0.06 m/s, and the SVE error statistic CEP value in the 2D horizontal direction is 0.04 m/s. When the VDSF-ARUKF method is used for the SVE, the results of the SVE in the X, Y, Z directions of the ECEF coordinate system are shown in Figure 7.

Comparing the statistical results of different SVE methods in Table 1, it can be seen that, for the carrier in the low-dynamic scene, the SVE accuracy in the 2D horizontal direction and in the 3D direction using the VDSF-ARUKF method are higher than that of using the ARUKF method based on the CPDD observation. The accuracy of the 3D
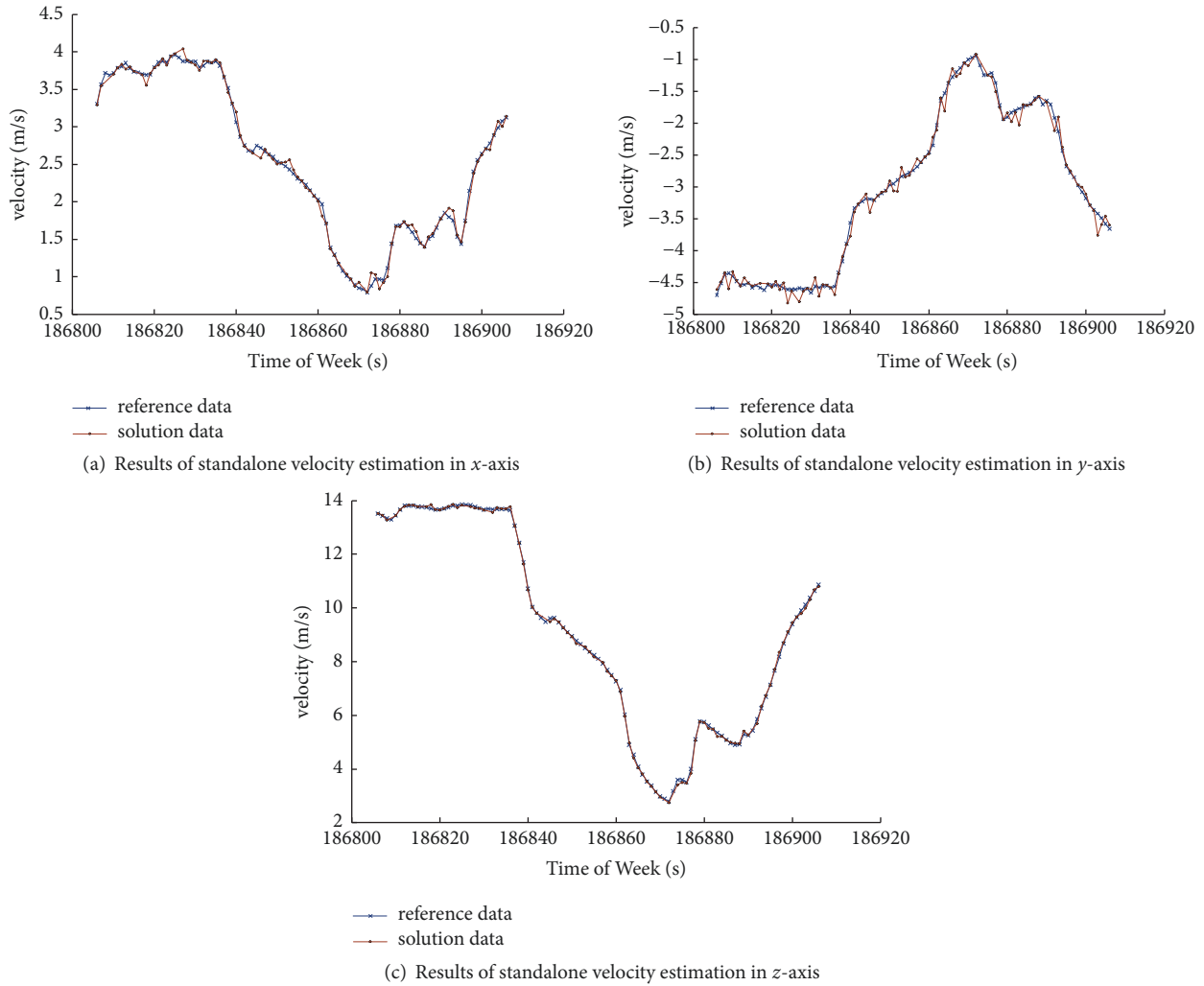
(a) Results of standalone velocity estimation in x-axis

(b) Results of standalone velocity estimation in y-axis

(c) Results of standalone velocity estimation in z-axis

FIGURE 6: Velocity estimation results of the VDFF-ARUKF navigation solution method.

velocity estimation results of the VDSF-ARUKF method reaches the order of several 10^{-2} m/s.

In the X, Y, and Z directions of the ECEF coordinate system, comparing SVE results shown in Figure 7 with the SVE results in Figure 5, it can be seen that the SVE results of the VDSF-ARUKF method in the X, Y, and Z directions are better than those of the ARUKF navigation solution method based on the CPDD observations. Integrating the raw Doppler SVE results by the velocity domain selection fusion strategy, the problem of the accuracy decrease of the SVE results, or even that the normal SVE cannot be performed caused by the data quality problem of the CPDD observations, can be solved. Comparing with the results in Figures 5 and 6, it can be seen that the curve of the SVE results obtained by using the VDSF-ARUKF method is smoother and without big fluctuation, and the VDSF-ARUKF method can track the dynamic change of the system better. Therefore, the results of using the VDSF-ARUKF method in the velocity domain are more accurate than those of using the VDFF-ARUKF method.

In order to verify that the proposed VDSF-ARUKF method can improve the reliability of the CPDD standalone velocity estimation results, a verification experiment configured as follows is used. The observation data in the verification experiment are recorded in the ground car testing experiment in Guangzhou city. The multidimensional gross errors of the CPDD observations are simulated in the beginning epochs of the selected testing data; that is, the gross errors are inserted every 3 observation epochs into the carrier-phase observations corresponding to the 4 selected BeiDou satellites. The simulation of the gross errors is implemented as small cycle slips of the carrier-phase observations. The occurrence of multidimensional gross errors in the CPDD observations will lead to a decrease in the reliability of the high-precision SVE method based on the ARUKF. The reliability of the ARUKF SVE method can be improved by the proposed VDSF strategy. Three kinds of SVE methods are used to perform the SVE. These three methods are the CPDD SVE method based on the ARUKF method, the VDFF-ARUKF method, and the VDSF-ARUKF method.

TABLE 2: The SVE errors of three different filter-based SVE methods.

Method Type	CEP (m/s)	SEP (m/s)	error components in the E, N, U directions (m/s)		
			E	N	U
ARUKF using CPDD observation	0.15	0.31	0.04	0.22	0.07
VDFF-ARUKF	0.09	0.18	0.06	0.09	0.16
VDSF-ARUKF	0.05	0.07	0.01	0.06	0.03

(a) Results of standalone velocity estimation in x-axis

(b) Results of standalone velocity estimation in y-axis

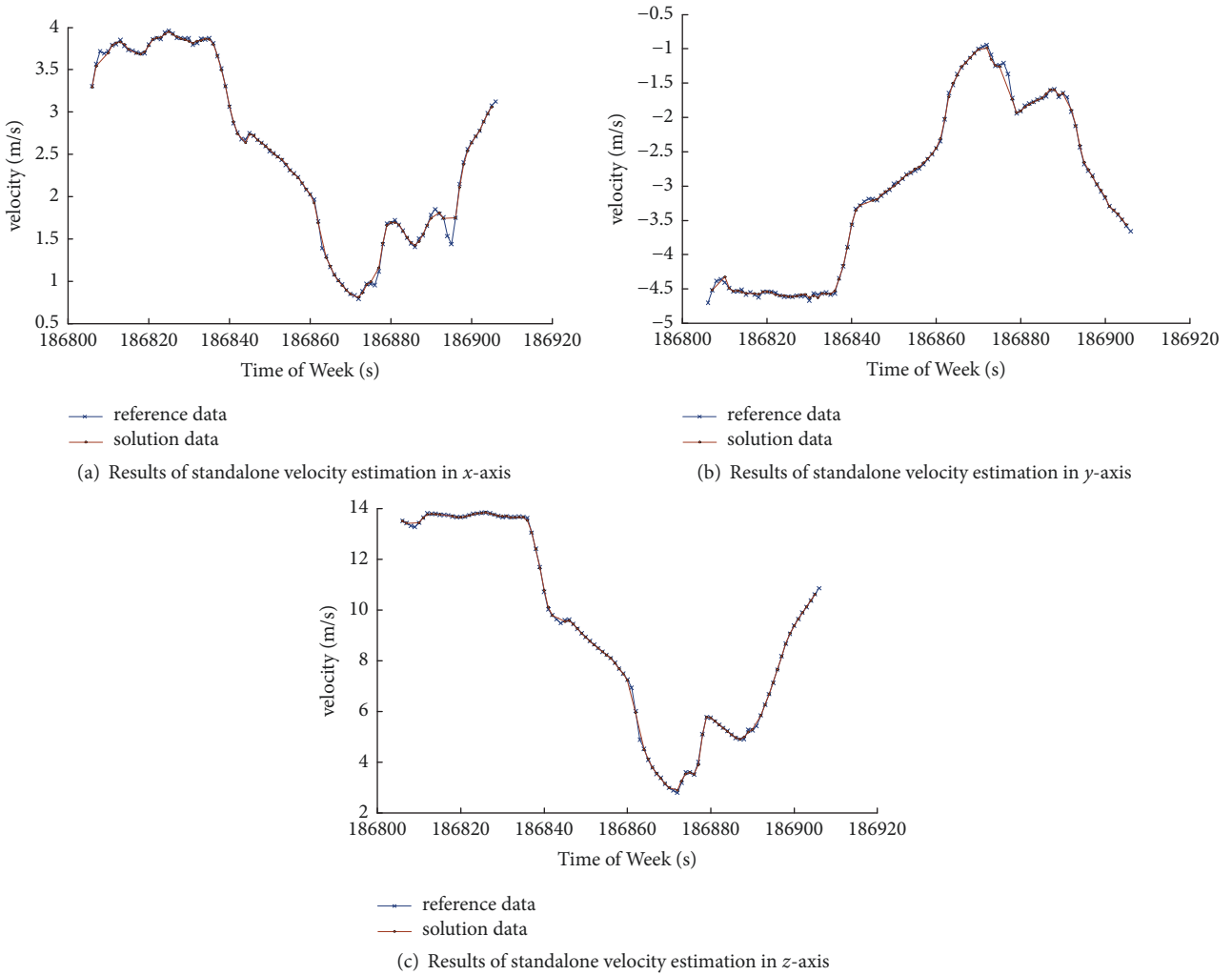(c) Results of standalone velocity estimation in z-axis

FIGURE 7: Velocity estimation results of the VDSF-ARUKF navigation solution method.

Based on the high-precision SVE results of the GPS/INS integrated navigation system, the error of the reference SVE results is about 0.03 m/s. The errors of these three different filter-based SVE methods are calculated separately. The error statistics of the SVE results are shown in Table 2.

It can be seen from Table 2 that when multidimensional gross errors occur in the CPDD observation, if the ARUKF method using the CPDD observation is applied to the velocity estimation, the SVE error will increase from the order of several 10^{-2}m/s to the order of several 10^{-1}m/s, the

corresponding 3D SVE error is about 0.31 m/s. If the SVE is performed using the VDFF-ARUKF method, the obtained SVE errors are smaller than those of the ARUKF method using the CPDD observation. The SVE error statistics can be used to evaluate the reliability of the ARUKF method, the VDFF-ARUKF method, and the VDSF-ARUKF method. The reliability of the VDFF-ARUKF method is higher than that of the ARUKF method using the CPDD observation. Among them, the SVE error of the VDFF-ARUKF method in the 3D direction is about 0.18 m/s, and the SVE error of the

VDFF-ARUKF method in the 2D horizontal direction is 0.09 m/s. The SVE errors of the VDFF-ARUKF method in the E direction and the N direction of the ENU coordinate system are all on the order of several 10^{-2} m/s, and the SVE error in the U direction is greater than that of the ARUKF SVE method using the CPDD observation. However, when there are multidimensional gross errors of the CPDD observation in the partial testing epochs, the SVE errors of the VDSF-ARUKF method can be obtained. The SVE error of the VDSF-ARUKF method in the 3D direction is 0.07 m/s. The SVE error of the VDSF-ARUKF method in the 2D horizontal direction is about 0.05 m/s. The above experimental results show that the reliability of the VDSF-ARUKF method is the highest among these three different filter-based SVE methods. The reliability of the VDFF-ARUKF method is ranked as the second, and the reliability of the ARUKF method using the CPDD observation is the lowest.

4. Conclusion

This paper analyzes the accuracy and reliability of different filter-based SVE methods for the BDS receiver and proposes the VDSF-ARUKF method for standalone velocity estimation, which can be seen as an improved ARUKF method based on the VDSF strategy. The effectiveness of this improved ARUKF method is verified by using the actual observation of the self-developed BDS receiver. The main work of this paper is as follows.

Based on the idea of data fusion, the accuracy and reliability of the corresponding SVE results of the original ARUKF method can be improved with the VDSF-ARUKF method, which combines the SVE results using two different kinds of Doppler observations. According to the SVE results of the verification experiments, the accuracy of the VDSF-ARUKF method proposed in this paper is on the order of several 10^{-2} m/s, which can significantly improve the accuracy and reliability of the original ARUKF method using the CPDD observations in the velocity domain. The SVE accuracy of the VDSF-ARUKF method is higher than that of the VDFF-ARUKF method and the ARUKF method using the CPDD observations. In the case of multidimensional gross errors in the CPDD observations, the VDSF-ARUKF method can still obtain the SVE results with the highest accuracy on the order of several 10^{-2} m/s compared with the VDFF-ARUKF method and the ARUKF method using CPDD observations.

The combination of the error detection method based on the posterior residual χ^2 and the robust filtering based on the Huber robust equivalence weight function can simultaneously improve the error suppression ability of the UKF filter for both big and small gross errors and improve the numerical stability and dynamic system tracking characteristics of the UKF navigation solution method in the dynamic scenes.

In this paper, the improved ARUKF method based on VDSF strategy has some shortcomings. For example, limited by the available experimental environment, the prototype program in this paper can be only implemented on the PC platform. Therefore, the corresponding SVE results only reflect the performance evaluation results within the offline analysis. In addition, the real testing scenario, such as the low-dynamic car testing experiments, and the limited experimental data also limit the evaluation of the method performance. But these results can also provide some guidelines for the future work. In order to evaluate the performance of the improved ARUKF method in the actual scene, our next step is to port the prototype program to the platform of the real BDS receiver. Besides, more data characteristics, such as the interfrequency deviation, need to be considered for the multifrequency BDS receivers in the practical applications. In order to solve the problem of accuracy and reliability improvement of the ARUKF SVE method, the redundant information can provide some enlightenment for future BDS solutions.

Abbreviations

The following abbreviations are used in this manuscript:

ARUKF:	Adaptively Robust Unscented Kalman Filter
BDS:	BeiDou Navigation Satellite System
CPDD:	Carrier-Phase-Derived Doppler
CEP:	Circular error probable
ECEF:	Earth Centered Earth Fixed
ENU:	East North Up
GPS:	Global positioning system
GPST:	Global positioning system time
GNSS:	Global Navigation Satellite Systems
GEO:	Geostationary earth orbit
IGSO:	Inclined geostationary satellite orbit
ICD:	Interface control document
MEO:	Medium earth orbit
PNT:	Positioning, navigation, and timing
RD:	Raw Doppler
RMS:	Root mean square
SVE:	Standalone velocity estimation
SEP:	Spherical error probable
TOW:	Time of week
UAV:	Unmanned aerial vehicles
UKF:	Unscented Kalman Filter
VDSF:	Velocity Domain Selective Fusion
VDFF:	Velocity Domain Fault-tolerant Federated
VDSF-ARUKF:	Velocity Domain Selective Fusion Adaptively Robust UKF
VDFF-ARUKF:	Velocity Domain Fault-tolerant Federated Adaptively Robust UKF
2-D:	Two-dimensional
3-D:	Three-dimensional
WLS:	Weighted Least Square.

Data Availability

The datasets generated during the current study are available from the corresponding author on reasonable request.

Conflicts of Interest

The authors declare no conflicts of interest.

Acknowledgments

References

[1] H. He, *Precise Kinematic GPS Surveying and Quality Control*, Information Engineering University, Zhengzhou, China, 2002.

[2] D. Salazar, M. Hernandez-Pajares, J. M. Juan-Zornoza, J. Sanz-Subirana, and A. Aragon-Angel, "EVA: GPS-based extended velocity and acceleration determination," *Journal of Geodesy*, vol. 85, no. 6, pp. 329–340, 2011.

[3] S. L. Kennedy, *Acceleration Estimation from GPS Carrier Phases for Airborne Gravimetry*, University of Calgary, Calgary, Italy, 2002.

[4] H. Kaifei, *GNSS kinematic position and velocity determination for airborne gravimetry*, GFZ German Research Centre for Geosciences, 2015.

[5] Q. Wang and T. Xu, "Combining GPS carrier phase and doppler observations for precise velocity determination," *Science China Physics, Mechanics & Astronomy*, vol. 54, no. 6, pp. 1022–1028, 2011.

[6] P. Wu, X. Ouyang, W. Liu, and F. Wang, "A positioning method of bds receiver under weak signal circumstances based on compressed fractional-step," *Tehnički Vjesnik*, vol. 21, no. 1, pp. 43–48, 2014.

[7] H. Kuusniemi, G. Lachapelle, and J. H. Takala, "Position and velocity reliability testing in degraded GPS signal environments," *GPS Solutions*, vol. 8, no. 4, pp. 226–237, 2004.

[8] K. Zheng, Z. Liu, X. Xiao, and X. Zhang, "Method of multi-dimensional gross errors snooping of GPS velocity estimation in airborne gravimetry," *Acta Geodaetica et Cartographica Sinica*, vol. 45, no. 6, pp. 663–669, 2016.

[9] X. Zhang, B. Guo, F. Guo, and C. Du, "Influence of clock jump on the velocity and acceleration estimation with a single GPS receiver based on carrier-phase-derived Doppler," *GPS Solutions*, vol. 17, no. 4, pp. 549–559, 2013.

[10] China Satellite Navigation Office, *BeiDou Navigation Satellite System Signal In Space Interface Control Document Open Service Signal B3I (Version 1.0)*, 2018.

[11] W. Fumei, *Error Compensation and Extension Ofadaptive Filtering Theory in GNSS/INS Integrated Navigation [phd Thesis]*, Information Engineering University, Zhengzhou, China, 2010.

[12] X. Yun and X. Zheren, "Comparison between phase-rate and doppler to determine velocity," *Geomatics and Information Science of Wuhan University*, vol. 28, pp. 581–584, 2003.

[13] H. Haibo, Y. Yuanxi, and S. Zhongmiao, "A comparison of several approaches for velocity determination with GPS," *Acta Geodaetica Et Cartographica Sinica*, vol. 31, pp. 217–221, 2002.

[14] Y. Chen, X. Yu, C. Ye, and M. Zhang, "Analysis of single-point GPS velocity determination with doppler," *Gnss World of China*, no. 1, pp. 31–34, 2008.

[15] S. Tan, *The Engineering of Satellite Navigation and Positioning*, National Defend Industry Press, Beijing, China, 2nd edition, 2010.

[16] S. Tan, "Innovative development and forecast of BeiDou system," *Acta Geodaetica et Cartographica Sinica*, vol. 46, no. 10, pp. 1284–1289, 2017.

[17] S. Ye, Y. Yan, and D. Chen, "Performance analysis of velocity estimation with BDS," *Journal of Navigation*, vol. 70, no. 3, pp. 580–594, 2017.

[18] F. Wang, X. Zhang, and J. Huang, "Error analysis and accuracy assessment of GPS absolute velocity determination with SA off," *Geomatics and Information Science of Wuhan University*, vol. 32, no. 6, pp. 515–519, 2007.

[19] Z. Shen, J. Peng, W. Liu, and F. Wang, "Analysis and accuracy assessment of standalone velocity determination methods with BDS receivers," in *Proceedings of the 2nd International Conference on Information Engineering*, Shenyang, China, 2017.

[20] X. Wang, W. Liu, B. Li, and G. Sun, "Detection and repair of cycle slips for undifferenced BDS triple-frequency observations," *Guofang Keji Daxue Xuebao/Journal of National University of Defense Technology*, vol. 38, no. 3, pp. 12–18, 2016.

[21] M. E. Cannon, G. Lachapelle, M. Szarmes, J. Hebert, J. Keith, and S. Jokerst, "DGPS kinematic carrier phase signal simulation analysis for precise velocity and position determination," *Journal of the Institute of Navigation*, vol. 44, pp. 231–246, 1997.

[22] X. Gong, R. Zhang, and J. Fang, "Application of unscented R-T-S smoothing on INS/GPS integration system post processing for airborne earth observation," *Measurement*, vol. 46, no. 3, pp. 1074–1083, 2013.

[23] X. Gong, W. Fan, and J. Fang, "Application of unscented R-T-S smoothing based on novel mathematical model in SINS/GPS integrated system post processing," *Measurement*, vol. 55, pp. 581–592, 2014.

[24] Y. Yang and X. Cui, "Adaptively robust filter with multi adaptive factors," *Survey Review*, vol. 40, no. 309, pp. 260–270, 2008.

[25] X. Cui and Y. Yang, "Adaptively robust filtering with classified adaptive factors," *Progress in Natural Science: Materials International*, vol. 16, no. 8, pp. 846–851, 2006.

[26] Y. Yang, H. He, and G. Xu, "Adaptively robust filtering for kinematic geodetic positioning," *Journal of Geodesy*, vol. 75, no. 2-3, pp. 109–116, 2001.

[27] L. Chang, B. Hu, G. Chang, and A. Li, "Huber-based novel robust unscented Kalman filter," *IET Science, Measurement & Technology*, vol. 6, no. 6, pp. 502–509, 2012.

[28] Y. Yang and J. Xu, "GNSS receiver autonomous integrity monitoring (RAIM) algorithm based on robust estimation," *Geodesy and Geodynamics*, vol. 7, no. 2, pp. 117–123, 2016.

[29] J. Liu, D. Li, and Z. Xiong, "Research on an improved residual chi-square fault detection method for federated unscented kalman filter," *Chinese Journal of Scientific Instrument*, vol. 30, no. 12, pp. 2568–2573, 2009.

[30] Y. Han, H. Wen, Y. Zhang, G. Chen, and L. Zhou, "The application of robust adaptive kalman filter based on chi-square test in deformation monitoring," *Journal of Geodesy and Geodynamics*, vol. 37, no. 6, pp. 604–608, 2017.

[31] R. Wen, Q. Honglei, C. Li, and X. Peng, "Improved residual X^2 inspection in integrated navigation fault detection of application," *Electronic Measurement Technology*, vol. 35, no. 11, pp. 124–128, 2012.

[32] Y. Yang, "Robust least square solution for parameter adjustment model," *Bulletin of Surveying and Mapping*, no. 6, 1994.

[33] Y. Yang, *Adaptive Navigation and Kinematic Positioning*, Surveying and Mapping Press, Beijing, China, 2nd edition, 2017.

[34] J. Liu, *Principle and Method of GPS Satellite Navigation And Positioning*, Science Press, Beijing, China, 2nd edition, 2008.